Dapagliflozin: a Sodium-glucose Cotransporter 2 Inhibitor, Attenuates Angiotensin II-induced Cardiac Fibrotic Remodeling by Regulating TGFβ1/ Smad Signaling

Yuze Zhang
Cardiovascular Department, The First Affiliated Hospital of Fujian Medical University
Xiaoyan Lin
Echocardiological Department, First Affiliated Hospital of Fujian Medical University
Yong Chu
Cardiovascular Department, First Affiliated Hospital of Fujian Medical University
Xiaoming Chen
Editorial Department of Chinese Journal of Hypertension
Heng Du
Cardiovascular Department, First Affiliated Hospital of Fujian Medical University
Hailin Zhang
Cardiovascular Department, First Affiliated Hospital of Fujian Medical University
Changsheng Xu
Cardiovascular Department, First Affiliated Hospital of Fujian Medical University
Hong Xie
Cardiovascular Department, First Affiliated Hospital of Fujian Medical University
Qinyun Ruan
Echocardiological department, First Affiliated Hospital of Fujian Medical University
Jinxiu Lin
Cardiovascular Department, First Affiliated Hospital of Fujian Medical University
Jie Liu
School of Pharmacy College of Xiamen University
Jinzhang Zeng
School of pharmacy College of Xiamen Universit
Ke Ma
Clinical Research Center, First Affiliated Hospital of Fujian Medical University
Dajun Chai (dajunchai@126.com)
Cardiovascular Department, The First Affiliated Hospital of Fujian Medical University
https://orcid.org/0000-0001-9477-9956

Original investigation

Keywords: Sodium-glucose cotransporter 2 inhibitors, Dapagliflozin, Angiotensin II, Cardiac fibrotic remodeling, TGFβ1/ Smad signaling

Posted Date: March 11th, 2021

DOI: https://doi.org/10.21203/rs.3.rs-288109/v1

Abstract

Background:

Cardiac remodeling is one of the major risk factors for heart failure. In patients with type 2 diabetes, sodium-glucose cotransporter 2 (SGLT2) inhibitors reduce the risk of the first hospitalization for heart failure, possibly through glucose-independent mechanisms, but the underlying mechanisms remain largely unknown. This study aimed to shed light on the efficacy of dapagliflozin in reducing cardiac remodeling and potential mechanisms.

Methods:

Sprague-Dawley (SD) rats, induced by chronic infusion of Angiotensin II (Ang II) at a dose of 520 ng/kg per minute for 4 weeks with ALZET® mini-osmotic pumps, were treated with either SGLT2 inhibitor dapagliflozin (DAPA) or vehicle alone. Echocardiography was performed to determine cardiac structure and function. Cardiac fibroblasts (CFs) were treated with Ang II with or without the indicated concentration of DAPA. The protein levels of collagen and TGF-β1/Smad signaling were measured along with body weight, and blood biochemical indexes.

Results:

DAPA treatment resulted in the amelioration of left ventricular dysfunction in Ang II-infused SD rats without affecting blood glucose and blood pressure. Myocardial hypertrophy, fibrosis and increased collagen synthesis caused by Ang II infusion were significantly inhibited by DAPA treatment. In *vitro*, DAPA inhibit the Ang II-induced collagen production of CFs. Immunoblot with heart tissue homogenates from chronic Ang II-infused rats revealed that DAPA inhibited the activation of TGF-β1/Smads signaling.

Conclusion:

DAPA ameliorates Ang II-induced cardiac remodeling by regulating the TGF-β1/Smad signaling in a glucose-independent manner. DAPA may serve as a novel therapy for pathological cardiac remodeling.

Introduction

Accentuated deposition of extracellular matrix (ECM) proteins contributed from cardiac fibroblasts (CFs) activation is a key feature of pathological myocardial remodeling involved in nearly all etiologies of heart diseases, which increases myocardial stiffness and ultimately leads to the progression of heart failure [1]. In the myocardium's fibrotic remodeling, activated CFs typically undergo myofibroblast transdifferentiation, expressing contractile proteins, such as α-smooth muscle actin (α-SMA), and synthesizing large amounts of structural ECM proteins mainly including types I and type III fibrillar collagen [2, 3]. Several mediators promote the development of cardiac fibrosis regardless of the underlying pathology and initiate factors. Angiotensin II (Ang II), the major effector in the renin-angiotensin–aldosterone system (RAAS), serves as a potent activating stimulus for cardiac fibrosis and

cardiomyocyte hypertrophy [4]. The chronic subjection model to Ang II in murine is widely used to mimic chronic hypertension upon neurohumoral activation, where reactive interstitial and perivascular fibrosis were observed [5]. Among a wide range of fibrogenic signaling pathways, transforming growth factor-β1 (TGF-β1)/Smad is crucial for the induction and maintenance of CFs activation and collagen synthesis, which partially mediates Ang II-induced structural remodeling [6].The strategies to reverse myocardial remodeling are now widely used as clinical interventions for treating heart diseases, and novel pharmacological targets are emerging [7]. In recent years, studies have revealed that sodium-glucose cotransporter 2 inhibitors (SGLT2i), a new class of anti-diabetic drugs, could play a cardioprotective role beyond the glucose-lowering effect [8]. In DAPA-HF (Dapagliflozin in Patients with Heart Failure and Reduced Ejection Fraction) trial, among patients with heart failure and a reduced ejection fraction, dapagliflozin (DAPA) reduced the risk of worsening heart failure or cardiovascular death, regardless of the presence or absence of diabetes [9]. In rats with cardiac ischemia/reperfusion injury, DAPA administration attenuated infarct size, decreased cardiac apoptosis, and improved cardiac mitochondrial function, leading to the improvement of left ventricular (LV) function [10]. Empagliflozin (EMPA; another SGLT2i) has been reported to improve LV ejection fraction and cardiac remodeling associated with improvements in cardiac metabolism and cardiac ATP production in myocardial infarction rats models [11].

Furthermore, experiment with human cardiac myofibroblast and found that EMPA can attenuate TGFβ1-induced fibroblast activation and cell-mediated collagen remodeling [12]. In general, there are relatively fewer studies concerning the cardioprotective potential of SGLT2i on patients with non-diabetic cardiovascular disease. And more histopathological evidence from animal models is needed to prove the effect of SGLT2i in alleviating cardiac fibrotic remodeling. Besides, the possible mechanisms by which SGLT2i achieve cardiovascular benefits remain to be elucidated since it's known that SGLT2 has no expression in the human heart [13].

Therefore, we performed the present study to confirm the glycemic-control-independent effect of DAPA towards cardiac remodeling using rats with chronic Ang II perfusion and explore the regulatory signaling with a focus on the TGF-β pathway. Our data suggeted that DAPA may help prevent patients from heart failure without diabetes and revealed possible mechanisms of the cardioprotective effects of SGLT2i.

Materials And Methods

Modeling and grouping

Eight-week-old male Sprague-Dawley (SD) rats (180 ± 20 g) purchased from Shanghai Laboratory Animal Center. All animals were housed in a room under temperature control at 23 ℃ and kept on a 12 h light/dark cycle. Commercial chow and water were supplied ad libitum. The animal experiment was completed in the Central Laboratory of the First Affiliated Hospital of Fujian Medical University. Twenty-four rats were randomly allocated into four groups (n = 6 for each group) were randomly divided into the following four groups: Control saline infusion group (CTL); Control treated with dapagliflozin group (5 mg/kg/day[14]) (CTL + DAPA); Ang II infusion with vehicle (0.9% sterile saline) gavage group (Ang II); Ang

II infusion with DAPA gavage group (Ang II + DAPA). Ang II (520 ng/kg/min, A9525, Sigma-Aldrich, St Louis, MO) or saline was continuously infused into rats through the osmotic pump (ALZET® Osmotic Pumps 2006, DURECT) for 4 weeks[15]. We administered the DAPA (gift of Astra Zeneca) or 0.9% sterile saline by gastric gavage continued up to 4 weeks. At the end of the treatment, blood pressure (BP) and body weight were measured, and then rats were anesthetized, echocardiography was performed to determine cardiac structure and function, blood samples and the heart were collected.

BP measurement

After completing 4-week drug administrations, BP was measured using a non-invasive tail-cuff system (Softron BP-2010A, Beijing Biotechnology Co., Ltd., Beijing, China). The BP data were collected three times under a resting state, and the average value was calculated.

Echocardiography

Four weeks after drug administrations, rats were anesthetized with 2% isoflurane via face mask. Transthoracic echocardiography (Vivid E9, GE Health-care, Diegem, Belgium) was performed using a 12S probe at frequencies of 4–12 MHz. M-mode images were obtained from papillary muscle levels to analyze the cardiac structure and function. Pulsed wave Doppler blood flow images of the apical four-chamber view at the mitral level and tissue Doppler images of the lateral and septal mitral annulus were recorded. Heart rate (HR) were recorded by synchronized electrocardiography. Images were quantified and analyzed by the Echopack 113.1.3 image analysis system (GE Healthcare). End-diastolic interventricular septum thickness (IVSd), end-diastolic left ventricular posterior wall thickness (LVPWd), and end-diastolic and end-systolic left ventricular internal diameters (LVIDd and LVIDs) were measured, and the left ventricular fractional shortening (LVFS) and the left ventricular ejection fraction (LVEF) were calculated as described previously [16]. The systolic peak velocities (s, s'), early diastolic peak velocities (e, e') and end-diastolic peak velocities (a, a') of the lateral and septal mitral annulus on the apical four-chamber view were measured using the quantitative tissue velocity imaging (QTVI) software (GE Healthcare). The systolic average peak velocity (S_{ave}), early diastolic average peak velocity (e_{ave}), late diastolic average peak velocity (a_{ave}) and the ratio of E/e_{eve} of the lateral and septal mitral annulus were calculated. All measurements were performed by an echocardiologist unaware of the identities of the experimental groups, and data recorded were averaged.

Measurements of laboratory chemistry and circulating bioactive peptides

After echocardiography was performed, blood samples were collected from the abdominal aorta and centrifuged to isolate serum and stored at -80 until assay. Glucose, lipid, blood urea nitrogen (BUN), serum creatinine (SCr) levels were measured by an enzymatic method and a urease colorimetric assay. Serum alanine aminotransferase (ALT)and aspartate aminotransferase (AST) levels were measured by a continuous monitoring method. Lactate dehydrogenase (LDH), creatine kinase (CK), and CK-MB were determined by the colorimetric method (Roche, Shanghai, China).

Circulating vasoactive peptide concentrations were determined using Enzyme-linked Immunosorbent Assay (ELISA) kits according to the manufacturer's protocol; the level of Atrial natriuretic peptide (ANP, Uscnk, Wuhan, China), Brain natriuretic peptide (BNP, Uscnk, Wuhan, China), Ang II (Cusabio Biotech, Wuhan, China), and Insulin (INS, Uscnk, Wuhan, China) were measured.

Histopathology

After blood samples were collected, the heart was anatomized, and the LVs were separated, blotted, and weighed. The heart weight to tibial length ratio (HW/TL, g/cm) and the LV weight to tibia length (LVW/TL, g/cm) ratio were calculated.

The heart tissues were fixed in 10% formalin for 24 h, dehydrated, embedded in paraffin, and sectioned at 5μm thickness, and these sections were mounted on glass slides. Hematoxylin-Eosin (H&E, Sigma-Aldrich, MO, USA) staining was used for histological analysis. Picric Acid-Sirius Red to assess the extent of fibrosis. Collagen was stained red. To quantify cardiomyocyte area and fibrotic percentage, the heart sections' images were obtained using an optical microscope and analyzed using Image-Pro Plus software version 6.0 (Media Cybernetics). Three sections were randomly selected from one heart of one rat in each group, and at least 6 views were analyzed.

Immunohistochemistry

For immunohistochemical staining, primary antibodies against Collagen I (Abcam, Cat no: ab34710), Collagen III (Abcam, Cat no: ab32854), α-smooth muscle actin (α-SMA) (Cell Signaling Technology, Cat no: #19245), TGF-β1 (ABclonal, Cat no: A2124) were used. Immunohistochemistry of cardiac sections was performed using a commercial immunohistochemical staining kit (Zhongshan Jinqiao Biotechnology, Beijing, China) following manufacturers' instructions. After counterstaining with hematoxylin, dehydration, the slides were observed in the light microscope. To semi-quantitate the targeted protein levels (brown color) in the hearts, all results were analyzed by Image-Pro Plus software 6.0 (Media Cybernetics). Three sections were randomly picked from 3 sections/heart/rat of 6 rats in each group were used for the study.

Cell culture and treatment

Primary cardiac fibroblasts (CFs) isolated from adult rat ventricular tissues as previously described [16]. Briefly, cells were grown in M199 medium (HyClone, Cat no: SH30253.01) (10 % fetal bovine serum and 1 % penicillin/streptomycin) at 5% CO_2, 37°C incubator. The purity of CFs in the culture was higher than 95% and only passages from 1 to 3 were used in the study to avoid age-dependent culture modifications. After incubation in a 0.5% fetal bovine serum M199 medium for 12 h, CFs were treated 24 h with 0.5, 1, 10 μM of Ang II (1μM) with or without DAPA (MedChemExpress, Cat no: HY-10450).

Immunoblot Analyses

Heart tissues and cell lysates were separated by 8–10% SDS-PAGE and transferred to nitrocellulose membranes. Antibodies used were rabbit polyclonal antibody against Collagen I (Abcam, Cat no:

ab34710), rabbit polyclonal antibody against Collagen III (Abcam, Cat no:ab32854), rabbit monoclonal antibodies against β-actin (Santa Cruz Biotechnology, Cat no: sc-47778), α-smooth muscle actin (α-SMA) (Cell Signaling Technology, Cat no: # 19245), Smad2 (Cell Signaling Technology, Cat no: #5339), Phospho-Smad2 (Cell Signaling Technology, Cat no: #18338), Smad3 (Sigma, Cat no: AV100621), Phospho-Smad3 (Sigma, Cat no: SAB4504210), Smad7 (Abcam, Cat no:ab216428) and rabbit polyclonal antibody against TGF-β1 (ABclonal, Cat no: A2124) at 4℃ overnight. The integrated density value of the target protein bands was measured by Image J software. β-actin was used to normalize the target protein level on the same blot.

Statistical Analysis

All results are expressed as the means ± SD, and all comparisons were analyzed using one-way ANOVA followed by the Student-Newman-Keuls test for multiple comparisons using IBM SPSS statistics 22 software. Results were considered significant when a value of $p < 0.05$ and values $p < 0.01$ were considered highly significant.

Results

Effects of DAPA on biochemical indicators and BP in rats

As shown in Table 1, there was no significant difference in the plasma glucose levels and insulin concentrations among the four groups throughout the study, indicating that our Ang II-infused rat model was free of diabetes. Compared to the CTL group, chronic perfusion of Ang II significantly increased SBP and DBP. In the Ang II + DAPA group, DAPA exerted no effect on SBP and DBP than the Ang II treated rats (Table 2). Chronic Ang II perfusion (5 mg/kg/day) significantly decreased body weight of rats after 4 weeks. During the experiment, there were no changes of total serum cholesterol (TC), triglyceride (TG), and low-density lipoprotein (LDL), and we did not find any liver, skeletal muscle, or kidney toxicity related to DAPA treatment (Table 1).

Table 1
Serum and biochemical indicators of Ang II rats treated with vehicle or DAPA for 4 weeks.

	CTL	CTL + DAPA	Ang II	Ang II + DAPA
Glu (mM)	8.29 ± 1.29	8.33 ± 1.28	8.09 ± 1.12	8.05 ± 1.17
INS (pg/ml)	223 ± 38.94	224.53 ± 66.16	205.95 ± 49.33	215.59 ± 43.51
TC (mM)	1.8 ± 0.2	1.6 ± 0.37	1.98 ± 0.48	1.85 ± 0.27
TG (mM)	1.14 ± 0.49	1.08 ± 0.46	1.31 ± 0.46	1.22 ± 0.56
LDL-C (mM)	0.35 ± 0.1	0.36 ± 0.09	0.35 ± 0.12	0.38 ± 0.07
HDL-C (mM)	0.53 ± 0.16	0.57 ± 0.05	0.51 ± 0.19	0.59 ± 0.1
ALT (U/l)	53.67 ± 8.59	61 ± 14.3	59.5 ± 7.61	52.33 ± 6.62
AST (U/l)	244.09 ± 10.05	246.16 ± 38.39	229.17 ± 17.41	236 ± 12.18
CK (U/l)	331.14 ± 11.81	327.08 ± 15.24	317.88 ± 18.12	321.81 ± 15.85
CK-MB (U/l)	338.28 ± 13.79	337.41 ± 15.76	318.38 ± 20.62	326.69 ± 16.81
LDH (U/l)	360.22 ± 13.26	359.74 ± 13.15	340.61 ± 24.75	354.96 ± 14.97
BUN (mM)	6.61 ± 1.43	6.88 ± 1.76	7.84 ± 2.13	8.64 ± 2.05
SCr (μmol/L)	18.12 ± 3.32	19.72 ± 2.89	20.05 ± 4.59	18.48 ± 2.59
UA (μmol/L)	11.3 ± 7.12	13.38 ± 5.86	8.22 ± 3.5	7.57 ± 3.95

Values are presented as mean ± SD (n = 6 rats per group). Abbreviations: Glu, glucose; INS, insulin; TC, total serum cholesterol, TG, triglyceride; LDL, low-density lipoprotein; HDL, high-density lipoprotein; SCr, serum creatinine; ALT, serum alanine aminotransferase; AST, aspartate aminotransferase; LDH, lactate dehydrogenase; CK, creatine kinase. Data are not significant for each group.

Table 2
Physical and conventional echocardiographic parameters in normal and Ang II-infused rats treated with vehicle or DAPA.

Parameters	CTL	CTL + DAPA	Ang II	Ang II + DAPA
BW (g)	362.17 ± 12.67	358 ± 9.93	320.33 ± 15.31*	318.5 ± 12.29*
SBP (mmHg)	131.95 ± 13.49	134.4 ± 16.43	228.28 ± 14.62*	222.67 ± 19.34*
BP (mmHg)	102.6 ± 16.62	106.77 ± 11.2	190.02 ± 18.49*	173.1 ± 17.58*
HW (g)	1.0 ± 0.08	1.03 ± 0.07	1.33 ± 0.05*	1.14 ± 0.1*†
LVW (g)	0.71 ± 0.07	0.71 ± 0.08	1.0 ± 0.03*	0.85 ± 0.07*†
IVSd (mm)	1.83 ± 0.08	1.82 ± 0.06	2.5 ± 0.14*	1.85 ± 0.09†
LVEDd (mm)	7.45 ± 0.65	7.49 ± 0.19	6.28 ± 0.42*	7.06 ± 0.71†
LVEDs (mm)	4.49 ± 0.26	4.37 ± 0.23	3.37 ± 0.23*	4.0 ± 0.5*†
LVPWd (mm)	1.68 ± 0.1	1.74 ± 0.13	2.32 ± 0.13*	1.73 ± 0.12†
LVEDV (ml)	0.94 ± 0.22	0.92 ± 0.05	0.58 ± 0.1*	0.81 ± 0.24†
LVESV (ml)	0.22 ± 0.04	0.2 ± 0.02	0.1 ± 0.02*	0.17 ± 0.07*†
LVEF (%)	75.47 ± 3.21	78.02 ± 2.57	82.88 ± 0.79*	79.9 ± 1.99*†
LVFS (%)	39.51 ± 2.83	40.61 ± 1.41	46.32 ± 0.85*	43.46 ± 1.79*†
HR	389.48 ± 21.59	377.53 ± 17.21	409.01 ± 26.04	409.32 ± 21.06

Values are presented as mean ± SD (n = 6 rats per group). Abbreviations: BW, body weight; SBP, systolic blood pressure; DBP, diastolic blood pressure; HW, heart weight; LVW, left ventricle weight; TL, tibia length; IVSd, End-diastole interventricular septum thickness; LVEDd, left ventricular end-diastolic dimension; LVEDs, left ventricular end-systolic dimension; LVEDV, left ventricular end-diastolic volume; LVESV, left ventricular end-systolic volume; LVPWd, diastolic left ventricular posterior wall thickness; LVFS, left ventricular fractional shortening; LVEF, the left ventricular ejection fraction; HR, Heart rate. Data are expressed as the mean ± SD. *$P < 0.05$ relative to CTL group. †$P < 0.05$ relative to Ang II group.

DAPA attenuated cardiac remodeling and improved cardiac dysfunction induced by Ang II in rats

To clarify the effect of DAPA on cardiac function in rats, Ang II (520ng/kg/min) or saline was continuously infused into rats, and rats were treated with DAPA (5 mg/kg/bw) or saline for 4 weeks. Chronic AngII infusion caused significant hypertrophy in comparison with control rats. As shown in Fig. 1C, Ang II infused rats showed increases in HW, HW/TL, LVW, and LVW/TL ratios ($P < 0.01$), and these

increases were significantly attenuated by DAPA ($P < 0.05$). Besides, we assessed the serum levels of ANP, BNP and Ang II using ELISA. The results showed that ANP, BNP, and Ang II were increased in Ang II group. DAPA treatment markedly reduced these parameters to some extent (Fig. 1A, B).

To assess the effects of DAPA on the cardiac structure and function in Ang II treated rats, we examined the rats with echocardiography. As shown in Table 2 and Fig. 1D, after Ang II infusion, LVEF and LVFS were significantly increased compared to control group (82.88 ± 0.79% vs 78.02 ± 2.57% and 46.32 ± 0.85% vs 40.61 ± 1.41% respectively, $P < 0.01$). In Ang II + DAPA group, LVEF and LVFS were significantly decreased compared to the Ang II group (79.9 ± 1.99% vs 82.88 ± 0.79% and 43.46 ± 1.79% vs 46.32 ± 0.85% respectively, $P < 0.05$). IVSd and LVPWd in Ang II- infused group were significantly increased than those in control group, and the LVEDd, LVEDs, end-diastolic volume (EDV), end-systolic volume (ESV) of Ang II-infused rats were significantly lower than those in control group. These results are consistent with previous reports [17, 18]. After DAPA treatment, these changes in Ang II treated rats were reversed substantially (Table 2).

QTVI has higher sensitivities in detecting cardiac function compared to conventional echocardiography. Therefore, we assessed early cardiac function changes in rats and the protective effects of DAPA using this technique. Interestingly, we found that compared with the control group, s, s', s_{ave}, e, e', e_{ave}, a, a' and a_{ave} in Ang II group were all significantly decreased ($P < 0.01$). Strikingly, DAPA treatment significantly increased s, s', s_{ave}, e, e', e_{ave}, a, a' and a_{ave} of Ang II-infused rats ($P < 0.05$), e and e_{ave} in Ang II+DAPA group were significantly higher than those in Ang II group. Furthermore, a_{ave}/e_{ave} and E/a_{ave} ratios in Ang II group were higher than those in control group (Table 3). These suggest that DAPA can attenuate cardiac remodeling and left ventricular dysfunction induced by Ang II infusion in rats.

Table 3
The effects of DAPA treatment on quantitative tissue velocity imaging parameters.

Parameters	CTL	CTL + DAPA	Ang II	Ang II + DAPA
s (mm/s)	2.68 ± 0.34	2.62 ± 0.28	1.66 ± 0.14*	1.96 ± 0.15†
a (mm/s)	1.87 ± 0.26	1.84 ± 0.22	1.38 ± 0.20*	1.66 ± 0.17†
e (mm/s)	2.89 ± 0.36	2.92 ± 0.44	1.84 ± 0.32*	2.66 ± 0.25†
a/e ratio	0.64 ± 0.12	0.63 ± 0.14	1.09 ± 0.13*	0.89 ± 0.11†
s'(mm/s)	2.64 ± 0.31	2.60 ± 0.22	1.58 ± 0.28*	2.09 ± 0.29†
a'(mm/s)	2.42 ± 0.23	2.46 ± 0.28	1.86 ± 0.23*	2.27 ± 0.21†
e'(mm/s)	3.74 ± 0.33	3.80 ± 0.42	2.21 ± 0.28*	2.86 ± 0.37#
a'/e' ratio	0.82 ± 0.12	0.80 ± 0.14	0.96 ± 0.10*	0.88 ± 0.08†
s_{ave}	2.92 ± 0.24	2.89 ± 0.28	1.67 ± 0.23*	2.19 ± 0.18†
a_{ave}	2.57 ± 0.60	2.47 ± 0.52	1.87 ± 0.36*	2.19 ± 0.34†
e_{ave}	3.67 ± 0.32	3.68 ± 0.28	1.92 ± 0.32*	2.64 ± 0.24†
a_{ave}/ e_{ave}	0.69 ± 0.14	0.68 ± 0.21	0.96 ± 0.21*	0.74 ± 0.27†
E/e_{ave}	28.68 ± 0.46	29.64 ± 0.48	46.24 ± 0.58*	36.49 ± 0.54†

Values are presented as mean ± SD (n = 6 rats per group). Abbreviations: s, peak systolic mitral annular velocity at lateral side; s', peak systolic mitral annular velocity at septal side; s_{ave}, average value of the peak systolic mitral annular velocity; a, late diastolic mitral annular velocity at lateral side; a', late diastolic mitral annular velocity at septal side; a_{ave}, average value of the late diastolic mitral annular velocity; e, early diastolic mitral annular velocity at the lateral side; *e*', early diastolic mitral annular velocity at the septal side; e_{ave}, average value of the early diastolic mitral annular velocity; E, Peak velocities of diastolic early transmitral Doppler flow; *P < 0.05 relative to CTL group; † P < 0.05 relative to Ang II group.

DAPA attenuates Ang II-induced cardiac hypertrophy.

As shown in Fig. 2, the Hematoxylin-Eosin (H&E) staining of the cross-section of the heart showed that the thickness of the ventricular wall (Fig. 2A) and cardiomyocyte cross-sectional areas (CSA) (Fig. 2B) were significantly increased in the Ang II group (P < 0.01), and these increases were significantly alleviated by DAPA (P < 0.05) (Fig. 2C). These results also confirmed the role of DAPA in Ang II-induced cardiomyocyte hypertrophy.

DAPA reduced Ang II-induced myocardial fibrosis

Picrosirius Red (PSR) staining showed that chronic Ang II infusion for 4 weeks significantly increased red-stained fibers in the shapes of bundles and sheets in the myocardial tissues of Ang II treated rats, DAPA treatment significantly lessened Ang II-induced cardiac fibrosis. The connective tissue fraction in Ang II group (17.27 ± 1.51) was higher than that in the control group (5.82 ± 0.83). However, DAPA treatment obviously reduced the Ang II-induce increase of connective tissue fraction (10.44 ± 1.19 vs 17.27 ± 1.51, $P < 0.01$; Fig. 3A and 3B).

ECM synthesis, including collagen and fibronectin, plays an crucial role in myocardial fibrosis. To evaluate the effect of DAPA on collagen synthesis, immunohistochemistry and Western blotting were performed. As shown in Fig. 3A and 3B, immunohistochemistry analysis demonstrated that α-SMA, type I and type III collagen were significantly increased in the myocardial tissue of the Ang II-infused rats. DAPA treatment markedly reduced the positive percentages of α-SMA, type I and type III collagen. Subsequently, we performed Western blotting to further confirm the above findings. Ang II also increased the expression of α-SMA, type I and type III collagen in the cardiac tissues, and these increases were significantly attenuated by DAPA (Fig. 3C). These results suggest that DAPA could effectively inhibit Ang II-induced myocardial fibrosis in rats.

In the adult heart, activated CFs also participate in the healing response after acute myocardial infarction and during chronic disease states characterized by augmented interstitial fibrosis and ventricular remodelling. A central cytokine involved in fibroblast activation, at least as defined in cultured fibroblasts, is transforming growth factor-β (TGF-β) [19, 20]. TGF-β and its downstream effectors constitute one of the most potent regulatory cascades for α-SMA gene expression and myofibroblast differentiation [21]. To further confirm the protective effect of DAPA in *vitro*, CFs were pretreated with different concentrations of DAPA for 1h, followed by incubation in 1 μM Ang II for 24 h. As shown in Fig. 3D, Ang II significantly increased the expression of α-SMA, TGFβ1, type I and type collagen in CFs, which was significantly compromised by DAPA treatment in a dose-dependent manner.

DAPA suppressed the activation of pro-fibrotic TGF-β1/Smad signaling in Ang II-infused rats

The members of the TGF-β superfamily are critical regulators of remodeling and fibrosis. TGF-βs are released and activated in injured tissues, bind to their receptors and transduce signals in part through activation of cascades involving a family of intracellular effectors the receptor-activated Smads (R-Smads) [22]. We therefore investigated the effects of DAPA treatment on TGF-β/Smads signaling. As shown in Fig. 4A, immunohistochemical staining showed increased TGF-β1 expression in the Ang II-infused group. Compared with the Ang II group, DAPA markedly reduced the expression of TGF-β1. Meanwhile, immunoblotting results demonstrated that TGF-β1 expression and the ratios of p-Smad2/Smad2 and p-Smad3/Smad3 experienced a significant up-regulation in response to Ang II. Whereas DAPA treatment significantly decreased Ang II-induced up-regulation of TGFβ1 levels and p-

Smad2/Smad2 and p-Smad3/Smad3 ratios. Smad7, a negative inhibitor of TGF-β1/Smad signaling, was decreased in the Ang II group and greatly increased by DAPA treatment. These suggest that inhibiting TGF-β1/Smad pathway is one of the potential mechanisms for DAPA to improve myocardial remodeling and function.

Discussion

In the present study, we evaluated the influence of the SGLT2i DAPA on Ang II-induced cardiac remodeling. In *vivo*, we found that DAPA treatment inhibited Ang II-induced cardiac hypertrophy, fibrosis, and dysfunction without affecting serum glucose and blood pressure levels,. In *vitro*, we confirmed that DAPA inhibited Ang II-induced collagen synthesis in CFs. Furthermore, we demonstrated an inhibitory role of DAPA on cardiac fibrosis by interfering with TGF-β1/Smads signaling cascades in myocardium. These results implied that DAPA can improve cardiac remodeling without diabetes, which provides evidence for the underway clinical trials and a basis for follow-up experiments.

DAPA is a newly oral antidiabetic drug of SGLT2i that enhances renal glucose excretion or glycosuria and reduces hyperglycemia [23, 24]. It is reported that lower risk of heart failure and death in patients initiated on SGLT2i versus other glucose-lowering drugs [25]. Interestingly, the significant cardioprotective effects of SGLT2i could not be attributed solely to their glucose-lowering effects. In DECLARE-TIMI 58 (Dapagliflozin Effect on Cardiovascular Events-Thrombolysis in Myocardial Infarction 58), DAPA reduced the composite end point of cardiovascular death/hospitalization for heart failure in a broad population of patients with type 2 diabetes mellitus [26]. In DAPA-HF (Dapagliflozin and Prevention of Adverse Outcomes in Heart Failure) trial, patients who received DAPA had a significant 26% reduction in the risk of cardiovascular death or worsening HF compared to those who received placebo, with an 18% reduction in the risk of cardiovascular death and allcause mortality[24]. These data indicating DAPA can exert cardiovascular protection beyond hypoglycemic effect. However, the precise impacts and mechanisms still need further exploration.

Perfusion of Ang II is a canonical method for establishing a model of cardiovascular disease [5]. To clarify the benefits of DAPA on myocardial remodeling, we used chronic Ang II-infused non-diabetic rat model in the study. As expected, DAPA significantly improves cardiac function without lowering blood glucose. Previous results have indicated that continuous Ang II infusion at a dose of 1000 ng/kg/min for 2 weeks increases EF% and FS%, while Ang II infusion for 4 weeks decreases EF% and FS% [17, 18]. Unlike these studies, a lower dose of Ang II perfusion for 4 weeks was used in our study. But, it still can be seen that Ang II-infusion increased EF% and FS% in rats. There may be two possible explanation for this, one is that Ang II induce myocardial hypertrophy leads to compensatory enhancement of myocardial contractility, the other is that conventional echocardiography can not detect the early early cardiac dysfunction.

QTVI takes high-frequency real-time images and is not affected by left ventricular preload and left atrial pressure, allowing detection of the early abnormalities of LV function [27]. While analyzing the QTVI

results in the current study, we unexpectedly found that the decline of s, s' and s_{ave} is earlier than EF in Ang II-infused rats (Table 3), further confirming that reduced systolic mitral annular peak velocity is a sensitive indicator of early subclinical systolic impairment. Early diastolic mitral annular motion velocities (e, e' and e_{ave}) are key indicators of active left ventricular myocardial relaxation, while changes in end-diastolic mitral annular motion velocities (a, a' and a_{ave}) are associated with left atrial contractility and left ventricular end-diastolic compliance [28, 29]. The ratio of early diastolic peak blood flow velocity (E) and e_{ave} (E/e_{ave}) is positively associated with left ventricular filling pressure and indirectly reflects left ventricular diastolic function [30]. In our study, the decrease in e, e', e_{ave}, a, a', a_{ave} and the increase in a'/e', a_{ave}/e_{ave} and E/e_{ave} ratio in Ang II-infused group indicated a reduction in left ventricular diastolic function at the early stage of Ang II-induced rats. Interestingly, treatment of the rats with DAPA significantly improved the above parameters reflecting the LV systolic and diastolic function (Table 3).

LV hypertrophy (LVH) and increased LV mass (LVM) are associated with an increased risk for heart failure and sudden cardiac death [31]. In DAPA-LVH trial (A randomized controlled trial of dapagliflozin on left ventricular hypertrophy in people with type two diabetes), DAPA treatment significantly reduced LVM in people with T2D and LVH. This reduction in LVM was accompanied by reductions in systolic BP, body weight, visceral and subcutaneous adipose tissue, insulin resistance, and hsCRP[32]. In our study, DAPA treatment markedly reduced HW, HW/TL and LVW/TL ratio, IVSd, LVPWd and cardiomyocyte cross-sectional area in Ang II-induced rats (Table 2 and Fig. 2). The regression of LVH suggests DAPA can initiate reverse remodelling and changes in left ventricular structure that may partly contribute to the cardio-protective effects of DAPA. Unlike previous studies, we did not find BP-lowering effect of DAPA in our research. This may be related to the limitations of using tail-cuff method to measured BP. The mechanism of BP reduction with SGLT2i is not fully understood but is thought to be related to weight reduction, modest diuretic effect, and potentially sodium depletion [33, 34].

Myocardial fibrosis, characterized by excess deposition of ECM and myofibroblast accumulation, is an integral feature of the remodelling of the failing heart [1, 35]. CFs play a paramount role in the repair and remodelling of the heart that occurs following myocardial infarction and pathological stress because of their exceptional plasticity to undergo conversions into myofibroblasts [36]. In this study, DAPA treatment for 4 weeks successfully reduced the cardiac fibrosis, the deposition of type I and type III collagen, and α-SMA induced by Ang II infusion. In *vitro*, DAPA also reduced Ang II-induced collagen synthesis in CFs (Fig. 3D). These are consistent with previous reports [11, 37–39]. Thus, inhibition of ECM synthesis and fibroblast-to-myofibroblast conversion may be the important mechanisms for DAPA to decrease myocardial fibrosis.

Secreted TGF-β1 and activation of Smad-dependent canonical pathway upon injury is the main inducer of ECM production and fibroblast-to-myofibroblast conversion [40, 41]. In our research, DAPA reduced the expression of TGF-β1 and the ratios of p-Smad2/Smad2 and p-Smad3/Smad3 in Ang II-infused rats. In addition, Smad7, the negative regulator of the TGF-β1/Smad pathway, was significantly increased by DAPA treatment (Fig. 5). These results demonstrate an inhibitory role of DAPA of cardiac hypertrophy and

fibrosis by interfering with TGFβ1/Smads signalling in the myocardium. Therefore, an emerging postulate is that SGLT2 inhibition, independent of hyperglycaemia, may have direct and favourable effects on cardiac fibroblast phenotype and function, one of the most important factors of heart failure. Nevertheless, a detailed mechanism by which DAPA regulates TGF-β1/Smad signaling needs further elucidation.

Conclusions

In conclusion, in this study, we showed that SGLT2 inhibitor DAPA attenuates myocardial hypertrophy, fibrosis and improve LV function in Ang II-infused rat model *via* negative regulation of TGF-β1/Smad signaling. Our data indicates DAPA is a potential therapeutic option for patients with Ang II-induced myocardial remodeling.

Abbreviations

SGLT2: sodium-glucose cotransporter 2; TGF-β: transforming growth factor-β; Glu: glucose; INS: insulin; TC: total serum cholesterol: TG: triglyceride; LDL: low-density lipoprotein; HDL: high-density lipoprotein; SCr: serum creatinine; ALT: serum alanine aminotransferase; AST: aspartate aminotransferase; LDH: lactate dehydrogenase; CK: creatine kinase; BW: body weight; SBP: systolic blood pressure; DBP: diastolic blood pressure; HW: heart weight; LVW: left ventricle weight; TL: tibia length; IVSd: End-diastole interventricular septum thickness; LVEDd: left ventricular end-diastolic dimension; LVEDs: left ventricular end-systolic dimension; LVEDV: left ventricular end-diastolic volume; LVESV: left ventricular end-systolic volume; LVPWd: diastolic left ventricular posterior wall thickness; LVFS: left ventricular fractional shortening; LVEF: the left ventricular ejection fraction; HR: Heart rate; SDS: sodium dodecyl sulphate; PAGE: polyacrylamide gel electrophoresis; SD: standard deviation.

Declarations

Acknowledgements

We thank Prof. Leng-Xi Fu of the Central Lab, The First Affiliated Hospital, Fujian Medical University for his sincere assistance.

Authors' Contribution

D.C., K.M, X.L., Y.Z., Y.C., X.C., H.D., and J.X.L. were in charge of conception, design, analysis and interpretation of data. X.L., Y.Z., Y.C. and H.D. performed the in vivo and in vitro experiments. X.C., H.Z., C.X., H.X., J.L., J.Z. J.x.L., and D.C. contributed reagents, materials and analytical tools for the study. X.L. and Q. R. performed ultrasonic examination and data interpretation. X.L., Y.Z., K.M. and D.C. wrote the paper. K.M. and D.C. have full access to the data and take responsibility for the integrity and accuracy of the data analysis.

Funding

This work was supported in part by the National Natural Science Foundation of China [grant number 81670368]; the Fujian Health Education Joint Research Project [grant number WKJ2016-2-10]

Availability of data and materials

All data and materials are available upon request.

Ethics approval and consent to participate

The experimental animal studies were approved by the Institutional Animal Care and Use Committee of Fujian Medical University.

Consent for publication

All authors have declared their consent for this publication.

Competing Interests

The authors declare that there are no competing interests associated with the manuscript.

References

1. Travers JG, Kamal FA, Robbins J, Yutzey KE, Blaxall BC: **Cardiac Fibrosis: The Fibroblast Awakens**. *Circ Res* 2016, **118**(6):1021-1040.
2. Li L, Zhao Q, Kong W: **Extracellular matrix remodeling and cardiac fibrosis**. *Matrix Biol* 2018, **68-69**:490-506.
3. Frangogiannis NG: **The Extracellular Matrix in Ischemic and Nonischemic Heart Failure**. *Circ Res* 2019, **125**(1):117-146.
4. Forrester SJ, Booz GW, Sigmund CD, Coffman TM, Kawai T, Rizzo V, Scalia R, Eguchi S: **Angiotensin II Signal Transduction: An Update on Mechanisms of Physiology and Pathophysiology**. *Physiol Rev* 2018, **98**(3):1627-1738.
5. Bacmeister L, Schwarzl M, Warnke S, Stoffers B, Blankenberg S, Westermann D, Lindner D: **Inflammation and fibrosis in murine models of heart failure**. *Basic Res Cardiol* 2019, **114**(3):19.
6. Frangogiannis N: **Cardiac fibrosis: Cell biological mechanisms, molecular pathways and therapeutic opportunities**. *Molecular aspects of medicine* 2019, **65**:70-99.
7. Gourdie RG, Dimmeler S, Kohl P: **Novel therapeutic strategies targeting fibroblasts and fibrosis in heart disease**. *Nat Rev Drug Discov* 2016, **15**(9):620-638.
8. Nakagawa Y, Kuwahara K: **Sodium-Glucose Cotransporter-2 inhibitors are potential therapeutic agents for treatment of non-diabetic heart failure patients**. *J Cardiol* 2020, **76**(2):123-131.

9. Petrie MC, Verma S, Docherty KF, Inzucchi SE, Anand I, Belohlavek J, Bohm M, Chiang CE, Chopra VK, de Boer RA *et al*: **Effect of Dapagliflozin on Worsening Heart Failure and Cardiovascular Death in Patients With Heart Failure With and Without Diabetes**. *JAMA* 2020, **323**(14):1353-1368.
10. Lahnwong S, Palee S, Apaijai N, Sriwichaiin S, Kerdphoo S, Jaiwongkam T, Chattipakorn SC, Chattipakorn N: **Acute dapagliflozin administration exerts cardioprotective effects in rats with cardiac ischemia/reperfusion injury**. *Cardiovasc Diabetol* 2020, **19**(1):91.
11. Yurista SR, Sillje HHW, Oberdorf-Maass SU, Schouten EM, Pavez Giani MG, Hillebrands JL, van Goor H, van Veldhuisen DJ, de Boer RA, Westenbrink BD: **Sodium-glucose co-transporter 2 inhibition with empagliflozin improves cardiac function in non-diabetic rats with left ventricular dysfunction after myocardial infarction**. *Eur J Heart Fail* 2019, **21**(7):862-873.
12. Kang S, Verma S, Hassanabad AF, Teng G, Belke DD, Dundas JA, Guzzardi DG, Svystonyuk DA, Pattar SS, Park DSJ *et al*: **Direct Effects of Empagliflozin on Extracellular Matrix Remodelling in Human Cardiac Myofibroblasts: Novel Translational Clues to Explain EMPA-REG OUTCOME Results**. *Can J Cardiol* 2020, **36**(4):543-553.
13. Cowie MR, Fisher M: **SGLT2 inhibitors: mechanisms of cardiovascular benefit beyond glycaemic control**. *Nat Rev Cardiol* 2020, **17**(12):761-772.
14. Durak A, Olgar Y, Degirmenci S, Akkus E, Tuncay E, Turan B: **A SGLT2 inhibitor dapagliflozin suppresses prolonged ventricular-repolarization through augmentation of mitochondrial function in insulin-resistant metabolic syndrome rats**. *Cardiovasc Diabetol* 2018, **17**(1):144.
15. Silva GB, Garvin JL: **Angiotensin II-dependent hypertension increases Na transport-related oxygen consumption by the thick ascending limb**. *Hypertension* 2008, **52**(6):1091-1098.
16. Chai D, Lin X, Zheng Q, Xu C, Xie H, Ruan Q, Lin J, Liu J, Zeng J: **Retinoid X receptor agonists attenuates cardiomyopathy in streptozotocin-induced type 1 diabetes through LKB1-dependent anti-fibrosis effects**. *Clin Sci (Lond)* 2020, **134**(6):609-628.
17. Ye S, Luo W, Khan ZA, Wu G, Xuan L, Shan P, Lin K, Chen T, Wang J, Hu X *et al*: **Celastrol Attenuates Angiotensin II-Induced Cardiac Remodeling by Targeting STAT3**. *Circ Res* 2020, **126**(8):1007-1023.
18. Wang L, Zhang YL, Lin QY, Liu Y, Guan XM, Ma XL, Cao HJ, Liu Y, Bai J, Xia YL *et al*: **CXCL1-CXCR2 axis mediates angiotensin II-induced cardiac hypertrophy and remodelling through regulation of monocyte infiltration**. *Eur Heart J* 2018, **39**(20):1818-1831.
19. Stempien-Otero A, Kim DH, Davis J: **Molecular networks underlying myofibroblast fate and fibrosis**. *J Mol Cell Cardiol* 2016, **97**:153-161.
20. Tallquist MD, Molkentin JD: **Redefining the identity of cardiac fibroblasts**. *Nat Rev Cardiol* 2017, **14**(8):484-491.
21. Wang Y, Mack JA, Maytin EV: **CD44 inhibits alpha-SMA gene expression via a novel G-actin/MRTF-mediated pathway that intersects with TGFbetaR/p38MAPK signaling in murine skin fibroblasts**. *J Biol Chem* 2019, **294**(34):12779-12794.
22. Hanna A, Humeres C, Frangogiannis NG: **The role of Smad signaling cascades in cardiac fibrosis**. *Cell Signal* 2021, **77**:109826.

23. Garcia-Ropero A, Badimon JJ, Santos-Gallego CG: **The pharmacokinetics and pharmacodynamics of SGLT2 inhibitors for type 2 diabetes mellitus: the latest developments**. *Expert Opin Drug Metab Toxicol* 2018, **14**(12):1287-1302.
24. McMurray JJV, Solomon SD, Inzucchi SE, Kober L, Kosiborod MN, Martinez FA, Ponikowski P, Sabatine MS, Anand IS, Belohlavek J *et al*: **Dapagliflozin in Patients with Heart Failure and Reduced Ejection Fraction**. *N Engl J Med* 2019, **381**(21):1995-2008.
25. Kosiborod M, Cavender MA, Fu AZ, Wilding JP, Khunti K, Holl RW, Norhammar A, Birkeland KI, Jorgensen ME, Thuresson M *et al*: **Lower Risk of Heart Failure and Death in Patients Initiated on Sodium-Glucose Cotransporter-2 Inhibitors Versus Other Glucose-Lowering Drugs: The CVD-REAL Study (Comparative Effectiveness of Cardiovascular Outcomes in New Users of Sodium-Glucose Cotransporter-2 Inhibitors)**. *Circulation* 2017, **136**(3):249-259.
26. Wiviott SD, Raz I, Bonaca MP, Mosenzon O, Kato ET, Cahn A, Silverman MG, Zelniker TA, Kuder JF, Murphy SA *et al*: **Dapagliflozin and Cardiovascular Outcomes in Type 2 Diabetes**. *N Engl J Med* 2019, **380**(4):347-357.
27. Pauliks L: **Tissue doppler myocardial velocity imaging in infants and children--a window into developmental changes of myocardial mechanics**. *Echocardiography* 2013, **30**(4):439-446.
28. Mitter SS, Shah SJ, Thomas JD: **A Test in Context: E/A and E/e' to Assess Diastolic Dysfunction and LV Filling Pressure**. *J Am Coll Cardiol* 2017, **69**(11):1451-1464.
29. Suzue M, Mori K, Inoue M, Hayabuchi Y, Nakagawa R, Kagami S: **Developmental changes in the left ventricular diastolic wall strain on M-mode echocardiography**. *J Echocardiogr* 2014, **12**(3):98-105.
30. Thijssen JM, de Korte CL: **Cardiological Ultrasound Imaging**. *Curr Pharm Des* 2014, **20**(39):6150-6161.
31. Drazner MH: **The progression of hypertensive heart disease**. *Circulation* 2011, **123**(3):327-334.
32. Brown AJM, Gandy S, McCrimmon R, Houston JG, Struthers AD, Lang CC: **A randomized controlled trial of dapagliflozin on left ventricular hypertrophy in people with type two diabetes: the DAPA-LVH trial**. *Eur Heart J* 2020, **41**(36):3421-3432.
33. Inzucchi SE, Zinman B, Wanner C, Ferrari R, Fitchett D, Hantel S, Espadero RM, Woerle HJ, Broedl UC, Johansen OE: **SGLT-2 inhibitors and cardiovascular risk: proposed pathways and review of ongoing outcome trials**. *Diab Vasc Dis Res* 2015, **12**(2):90-100.
34. Filippatos TD, Liontos A, Papakitsou I, Elisaf MS: **SGLT2 inhibitors and cardioprotection: a matter of debate and multiple hypotheses**. *Postgrad Med* 2019, **131**(2):82-88.
35. Kong P, Christia P, Frangogiannis NG: **The pathogenesis of cardiac fibrosis**. *Cell Mol Life Sci* 2014, **71**(4):549-574.
36. van den Borne SW, Diez J, Blankesteijn WM, Verjans J, Hofstra L, Narula J: **Myocardial remodeling after infarction: the role of myofibroblasts**. *Nat Rev Cardiol* 2010, **7**(1):30-37.
37. Ye Y, Jia X, Bajaj M, Birnbaum Y: **Dapagliflozin Attenuates Na(+)/H(+) Exchanger-1 in Cardiofibroblasts via AMPK Activation**. *Cardiovasc Drugs Ther* 2018, **32**(6):553-558.

38. Oh CM, Cho S, Jang JY, Kim H, Chun S, Choi M, Park S, Ko YG: **Cardioprotective Potential of an SGLT2 Inhibitor Against Doxorubicin-Induced Heart Failure**. *Korean Circ J* 2019, **49**(12):1183-1195.
39. Lee HC, Shiou YL, Jhuo SJ, Chang CY, Liu PL, Jhuang WJ, Dai ZK, Chen WY, Chen YF, Lee AS: **The sodium-glucose co-transporter 2 inhibitor empagliflozin attenuates cardiac fibrosis and improves ventricular hemodynamics in hypertensive heart failure rats**. *Cardiovasc Diabetol* 2019, **18**(1):45.
40. Bujak M, Frangogiannis NG: **The role of TGF-beta signaling in myocardial infarction and cardiac remodeling**. *Cardiovasc Res* 2007, **74**(2):184-195.
41. Rodriguez P, Sassi Y, Troncone L, Benard L, Ishikawa K, Gordon RE, Lamas S, Laborda J, Hajjar RJ, Lebeche D: **Deletion of delta-like 1 homologue accelerates fibroblast-myofibroblast differentiation and induces myocardial fibrosis**. *Eur Heart J* 2019, **40**(12):967-978.

Figure

Figure 5 not available with this version.

Figures

Figure 1

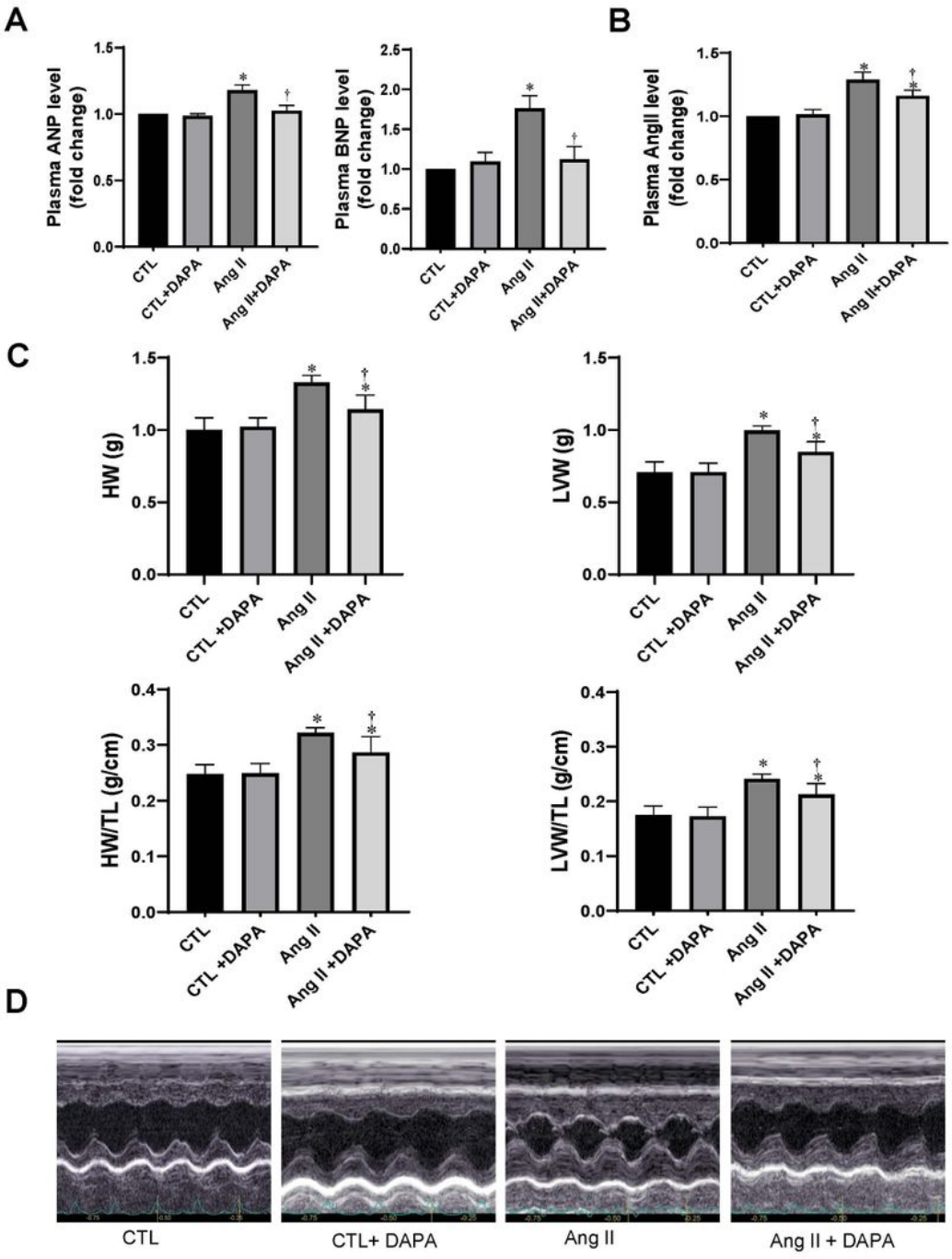

Figure 1

Administration of DAPA attenuates cardiac remodeling and improves cardiac dysfunction induced by Ang II in rats. (A, B) Analysis of ELISA of plasma ANP, BNP and Ang II levels; (C) HW, LVW, HW/TL ratios and HW/TL ratios; (D) Representative examples of M-mode echocardiography images. Data are expressed as the mean ± SD (n=6 rats per group). *P <0.05 relative to CTL group. †P <0.05 relative to Ang II group.

Figure 2

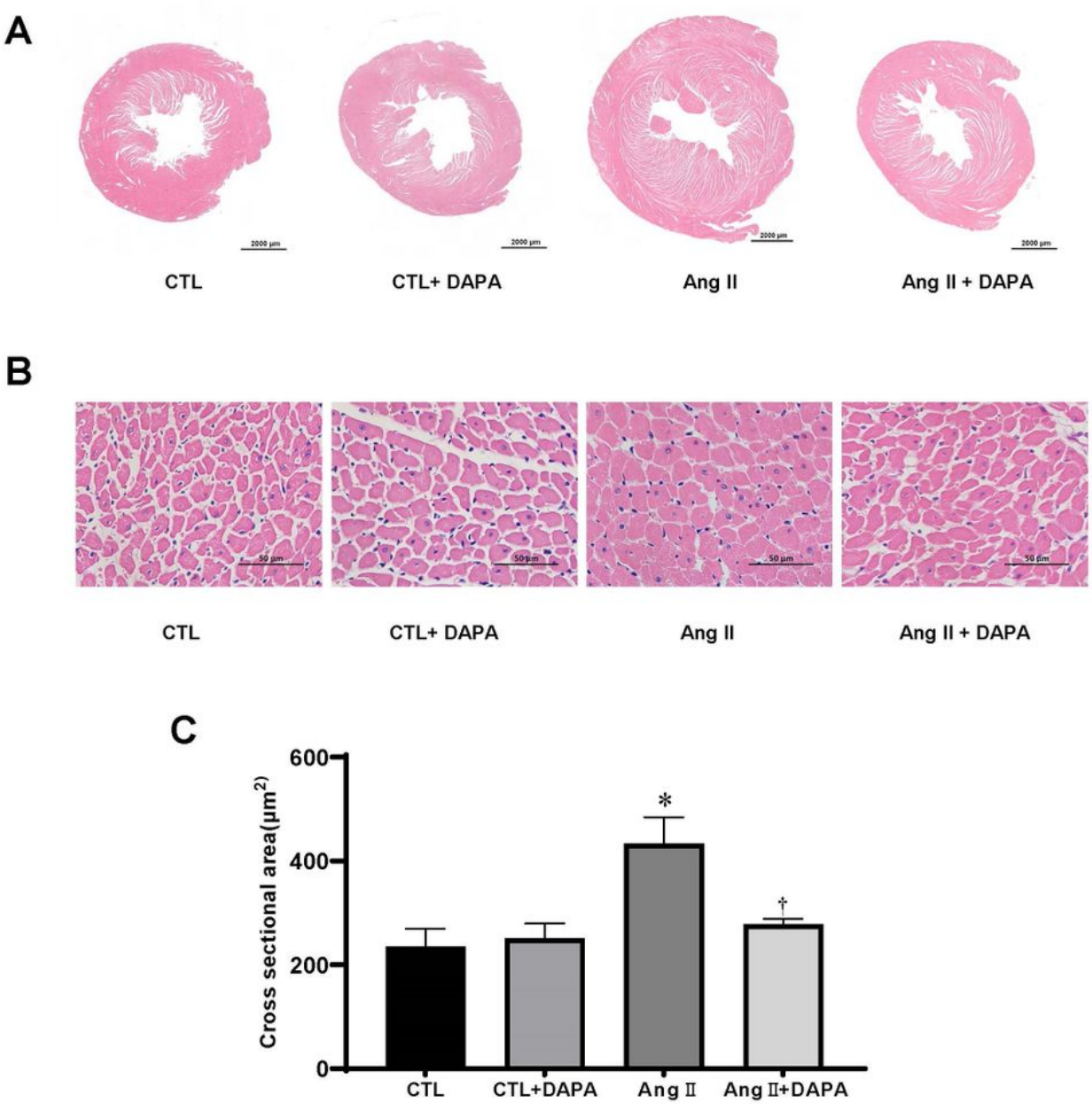

Figure 2

Administration of DAPA attenuates Ang II-induced cardiac hypertrophy. (A) H&E staining of the cross-section of the heart. Scale bar=2000μm; (B) The cardiomyocyte cross-section area (CSA) was stained with H&E staining. Scale bars=50μm; (C) Quantification of cardiomyocyte cross-section areas. Data are expressed as the mean ± SD (n=6 rats per group). *P <0.05 relative to CTL group. †P <0.05 relative to Ang II group.

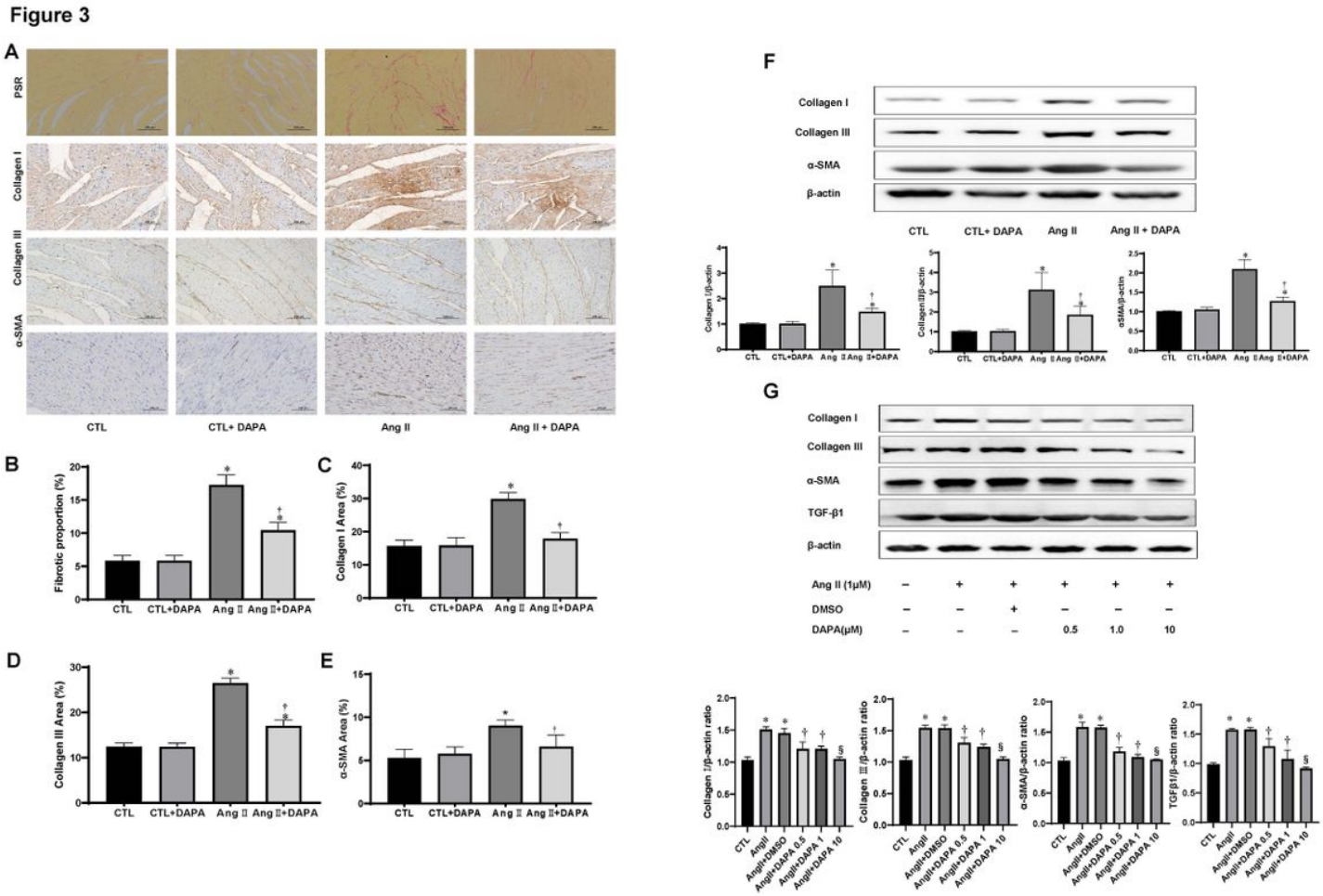

Figure 3

DAPA treatment suppresses matrix accumulation and myocardial fibrosis in vitro and in vivo. (A) The effects of DAPA on the fibrosis in myocardial tissue were observed by PSR staining (top), Scale bars=100μm; Red color represents collagen fibers deposition. Meanwhile, the expression of type I collagen, type III collagen and α-SMA (bottom) in the myocardium was detected by immunostaining and DAPI staining. Scale bars=100μm; (B) Quantification of red color in bar graph. OD values are presented as mean ± SD (n=6 rats per group). (C-E) Immunohistochemical analysis for the effect of DAPA on Ang II-induced expression of type I collagen, type III collagen and α-SMA in myocardial tissue. Values are presented as mean ± SD (n=6 rats per group). *P <0.05 relative to CTL group. †P <0.05 relative to Ang II group. (F) Effects of DAPA treatment on expression of type I collagen, type III collagen, α-SMA in Ang II-infused rats were examined by immunoblotting. The relative ratio of type I collagen, type III collagen, α-SMA over β-actin was determined by densitometric analysis respectively.Values are means±SD (n=3). *P <0.05 relative to CTL group. †P <0.05 relative to Ang II group. (G) DAPA inhibits Ang II-induced expression of type I collagen, type III collagen, α-SMA and TGF-β1 in CFs. CFs treated with the indicated concentrations of DAPA for 1h were exposed to Ang II for 24 hours. The relative ratio of type I collagen, type III collagen, α-SMA and TGF-β1 over β-actin was determined by densitometric analysis respectively.Values are means±SD (n=3). DMSO: Dimethyl sulfoxide. Values are means ± SD. *P <0.05 relative to CTL group. †P <0.05 relative to Ang II group.§ P <0.05 relative to Ang II plus DAPA 0.5 group.

Figure 4

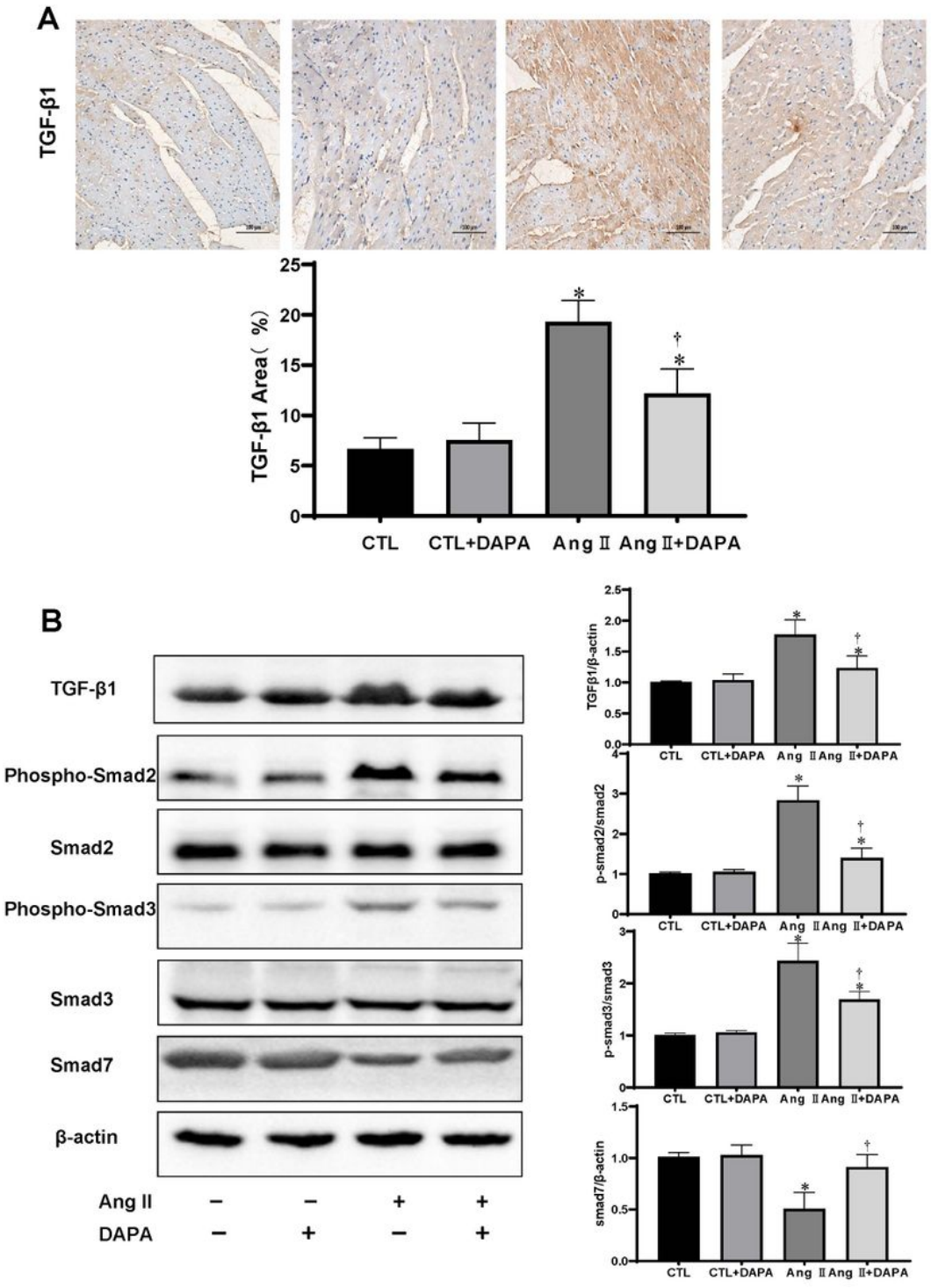

Figure 4

DAPA treatment inhibits the activation of the TGF-β1/Smad pathway in rats with continuous Ang II infusion. (A) Immunohistochemical analysis for the effect of DAPA on Ang II-induced expression of TGF-β1in myocardial tissue. Values are presented as means ± SD (n=6 rats per group). *P <0.05 relative to CTL group. †P <0.05 relative to Ang II group.Scale bars=100μm; (B) Inhibition of Ang II infusion -induced activation of TGF-β1/Smad pathway. The relative ratio of TGF-β1 and Smad7 over β-actin was

determined by densitometric analysis respectively. Also, the ratio of phosphor-Smad2/Smad2 and phosphor-Smad3/Smad3 was calculated based on densitometric analysis. Values are means±SD (n=3). *P <0.05 relative to CTL group. †P <0.05 relative to Ang II group.